P2.20 DIAGNOSIS OF CONDITIONAL MAXIMUM TORNADO DAMAGE PROBABILITIES

Bryan T. Smith[1], Richard L. Thompson[1], Harold E. Brooks[2], Andrew R. Dean[1], and Kimberly L. Elmore[2]

[1]NOAA/NWS/NCEP/Storm Prediction Center, Norman, Oklahoma
[2]NOAA/National Severe Storms Laboratory, Norman, Oklahoma

1. Introduction

Considerable effort in recent decades has focused on near-storm environment interrogation via model-based planar fields (e.g., Stensrud et al. 1997) and model-based proximity soundings in order to discriminate between nontornadic and significant (≥ F2) tornado environments for supercells (e.g., Thompson et al. 2003, hereafter T03; Thompson et al. 2007). This emphasis in severe environment discrimination led to the development of supercell ingredients-based composite parameters (i.e., significant tornado parameter, T03). Convective mode is an additional component widely recognized as a contributor to the occurrence and non-occurrence of severe weather. Recent work by Smith et al. (2012; hereafter S12) demonstrated the relationship of convective mode to tornado damage intensity, and Thompson et al. (2012; hereafter T12) took a step further and preliminarily investigated the relationship between convective mode, the near-storm environment, and tornado damage intensity.

The infusion of diagnostic parameters from objective hourly analyses, like the Storm Prediction Center's (SPC) mesoanalysis data (Bothwell et al. 2002), has contributed to greater awareness of potential tornado risk in a real-time operational forecast and warning setting (Glass 2011). Madsig (2008) discussed techniques to diagnose storm attributes via radar data and integration of environmental information into the warning decision making process. New work by Brotzge et al. (2012) revealed a clear relationship between tornado warning statistics and storm mode, suggesting that a combination of real-time convective mode, associated radar attributes (e.g., mesocyclone strength), and near-storm environment information may contribute to improved situational awareness of tornado impacts. A future Warn-On-Forecast concept has been proposed for operational meteorology (Stensrud et al. 2009) to mitigate loss accompanying severe storm hazards.

Recent tornado disasters [e.g., 26-27 April 2011, 22 May 2011; 24 May 2011, Ortega et al. (2012)] have supported an emphasis on assessing tornado threat to vulnerable populations. One such example involves several National Weather Service (NWS) local forecast offices tasked with issuing experimental impact-based severe thunderstorm and tornado warnings designed to convey the severe hazard (e.g., tornado), and its predicted impact on life and property, within the disseminated warning text.

This study builds upon previous work by S12 and T12 by further developing a multi-component dataset, including the use of peak lowest-level rotational velocity information, rather than mesocyclone nomograms (Andra 1997, Stumpf et al. 1998) to assess supercell mesocyclone circulation strength. In addition, other classifiable circulations [e.g., mesovortex; Trapp and Weisman (2003)] were also examined. The goal of this study is to combine near-storm environment information with real-time radar diagnosis to assess a maximum conditional tornado intensity risk.

In the following section, we detail the assigning of rotational velocity data and discuss the procedure used to develop conditional probabilistic tornado data. Results will be presented in section 3 with a discussion following in section 4.

2. Data and methodology

a. Data and event filtering

Radar-based convective modes, peak low-level rotational velocities, and near-storm environment data were assigned to a sample of tornadoes reported in the contiguous United States (CONUS) during 2009-2011 (i.e., ≥ EF2 from 2009-2010, and ≥ EF0 from 2011). The tornado segment

**Corresponding author address:* Bryan T. Smith, NOAA/NWS/NCEP/Storm Prediction Center, 120 David L. Boren Blvd., Suite 2300, Norman, OK 73072. Bryan.Smith@noaa.gov

data were filtered by the maximum EF-scale tornado event per hour on a 40 km Rapid Update Cycle (RUC; Benjamin et al. 2004) model horizontal grid, producing a sample of 1777 tornado grid-hour events. Convective mode was assigned to each tornado event via manual examination of full volumetric WSR-88D data (Section 2b) at the beginning time of each event, and peak low-level rotational velocity was calculated using super-resolution radar data (Torres and Curtis 2007) during the life span of each tornado event (Section 2c). Environmental information, consisting primarily of supercell-related convective parameters from the hourly SPC objective analyses, accompanied each grid-hour event.

Within the framework described above, the authors made careful manual adjustments to a small portion (6.7%) of the database. A large majority of suspected report errors involved incorrectly listed report times, as determined by time matching the reports to radar data. Examples of this suspected error type included reports well removed from existing radar echoes and time lagged on the order of tens of minutes to an hour or more. Offsets of one hour were relatively common near time zone boundaries. In situations where a suspected error could not be easily corrected, *Storm Data* was used to examine the description of the questionable reports in an effort to identify the storm responsible for the event.

b. Radar-based storm mode classification criteria

The Gibson Ridge radar-viewing software (http://www.grlevelx.com/) was used to analyze archived WSR-88D level-II or level-III single site radar data (Crum et al. 1993) from NCDC (http://www.ncdc.noaa.gov/nexradinv/) using the closest radar-site data (within 230 km of radar) to classify convective mode based on S12. Convective mode was determined using full volumetric radar data, especially when data through a deep layer were needed to perform a more thorough assessment of storm structure. Convective mode was assigned based on the volume scan and lower elevation tilts (e.g., 0.5 degree) of base reflectivity immediately prior to the time of the tornado event. If level-II data were unavailable, then level-III data were used. In situations when radar data were unavailable or incomplete, convective mode was not assigned (2 of 1777 events). Emphasis herein is placed on the 3 major convective mode classes: right-moving supercell (RM), quasi-linear convective system (QLCS), and disorganized (i.e., cells and clusters clearly not meeting QLCS or supercell criteria).

Discrete or embedded cells with focused areas of cyclonic (or anticyclonic) azimuthal shear were further scrutinized as potential supercells, following the mesocyclone nomograms developed by the Warning Decision Training Branch of the National Weather Service (NWS; after Andra 1997 and Stumpf et al. 1998). Supercells required a peak rotational velocity ≥ 10 m s^{-1} (i.e., a peak-to-peak azimuthal velocity difference of roughly 20 m s^{-1} over a distance of less than 10 km). Range dependence was included in the mesocyclone designation, per the 1, 2, and 3.5 nm mesocyclone nomograms.

QLCS is defined as consisting of contiguous reflectivity at or above the threshold of 35 dBZ for a horizontal distance of at least 100 km and a length-to-width aspect ratio of at least 3 to 1 at the time of the event, similar to Trapp et al. (2005). Disorganized storms were cellular modes that did not include supercell structures, and consisted mainly in conglomerates of storms meeting the reflectivity threshold but not satisfying either supercell or QLCS criteria. For a more thorough discussion pertaining to the complexity and challenges of categorizing convective mode, please refer to S12.

c. Low level rotational velocities

Peak inbound and outbound velocities were examined for each volume scan from immediately prior to tornado formation to immediately prior to tornado dissipation. Only velocity bins exhibiting cyclonic (anticyclonic) rotation within 5 mi and $\leq$ 45 degree angle from one another were considered, to avoid primarily convergent or divergent signatures. Only the highest peak inbound and outbound velocities were used to calculate the maximum rotational velocity [$Vrot = (|V_{in}| + |V_{out}|)/2$] from one volume scan, which was assigned to each tornadic event (Fig. 1). Ancillary data such as the time of the volume scan, elevation height above radar level (nearest 100 ft), and a subjective binary assessment if a clear/tight circulation was present were also recorded.

An overwhelming majority of events exhibited circulation diameters of a few miles or less—in some cases resolving the tornado circulation—but for a small percentage of cases (~ 12%), the Vrot diameter exceeded 3.5 mi. While many Vrot cases were easily assessed, Vrot identification at

times was a challenging task and involved considerable effort and uncertainty in assigning the peak inbound and peak outbound values. If tight circulation couplets (i.e., likely resolving the tornado vortex circulation) were clearly separate from other nearby higher velocity bins, these velocity data were recorded. Otherwise, preference was given to recording velocity bin information within the larger-scale circulation if these values were not more than 5 kts greater than Vrot of the inner circulation. Our manual analysis of velocity data is similar to techniques used in real-time warning decision-making. The subjective analysis used to diagnose circulation strength can be advantageous compared to an automated objective approach, especially in cases where radar is unable to resolve circulations [e.g., landspout; Brady and Szoke (1989)] or data is suspected of possible error. Using this approach, 1729 tornado events exhibited Vrot signatures with an identifiable circulation > 0 kt (Fig. 2).

While it was common for velocity signatures to vary considerably during the tornado event, it was uncommon for $\geq$ EF3 tornado events to display weak velocity values for most of the sampled volume scans. Many of the higher-end to extreme velocity cases exhibited consistent velocity values that were just below the peak rotational velocity value for a substantial part of the tornado segment grid hour (i.e., tornado event).

d. Conditional tornado probabilities

Probabilities of events in two-dimensional phase space were calculated by making kernel density estimates from the scatterplots, following Brooks (2009). A two-dimensional Gaussian kernel was applied to each possible category (e.g., EF1 tornadoes) and the standard deviation for the kernel was 5 kt and 1 for Vrot and STP, respectively. Only regions where there was a large enough density warranted the calculating of probabilities. It is important to note that, given the construction of the dataset, the exact numerical values of the probabilities should not be interpreted quantitatively for other datasets. The trends within individual figures are of importance, so that qualitative interpretation is possible.

3. Results

a. Peak low-level rotational velocities

A strikingly strong relationship exists between max Vrot and EF-scale for all convective modes. For higher EF-scale ratings, an increase in the max Vrot distribution occurred (Figs. 3–5). Substantial interquartile offset existed between several EF-scale rating classes, most notably between weak (EF0–EF1), strong (EF2–EF3), and violent tornado events (EF4–EF5). A largely monotonic increase is displayed for tornado events as EF-scale increases (Figs. 3–4) for events sampled below 6 000 ft above radar level (ARL), or within 62 nm of the radar site. See Fig. 6 for an approximate areal coverage of WSR-88D radar coverage below 3 000 ft and 6 000 ft (ROC 2012). For events sampled ≥ 6000' ARL, the interquartile overlap increased between EF3 and $\geq$ EF4 events. This result suggests that radar limitations in the form of larger beamwidth and reduced horizontal resolution lead to a degradation in the radar's ability to resolve stronger Vrot magnitudes for ≥ EF4 events at greater range from a radar site.

b. Convective mode and rotational velocity

S12 found variations in tornado EF-scale damage ratings were more closely related to mesocyclone strength than the specific type of RM (discrete, cluster, line). Hence, convective mode distributions investigated herein focused on differences between RM, QLCS, and disorganized storms. Based on the findings of S12, weak mesocyclones were most common with weak tornadoes (EF0-EF1), whereas strong mesocyclones were almost exclusively associated with EF3+ tornadoes when examining the volume scan prior to the tornado event. This study found a majority of events with weaker Vrot resulted in EF0–EF1 tornadoes (Fig. 7), whereas a larger fraction of total events (i.e., higher conditional probability) were EF2–EF5 tornado events as Vrot increased. Both RM and QLCS tornado event modes displayed a general increase in Vrot as EF-scale increased (Fig. 7). Around one quartile difference was found with RM amongst interquartile values of Vrot when compared to a ±1 RM EF-scale rating class (Fig. 7). Differences in mean Vrot values for ≥ EF4 vs. EF0, ≥ EF4 vs. EF2, and EF2 vs. EF0 were 39 kt, 26 kt, and 13 kt, respectively (Tables 1 and 2). All differences in EF-scale rating classes amongst RM were statistically significant at $\alpha < 0.001$ for a two-tailed *t* test with unequal variances (Table 3 ; Wilks 2006). A similar quartile difference is evident between QLCS EF0 and EF1 events and was also statistically significant at $\alpha < 0.001$ for a two-tailed t test (Table 4). RM tornado events were rated roughly one EF-scale less than QLCS tornado events with similar Vrot distributions.

QLCS tornadoes generally show weaker max Vrot values than RM tornadoes. Although several possible explanations for this are possible, the observed shallower vertical depth and smaller horizontal dimensions of the circulations may influence the ability of radars to resolve QLCS circulation strength relative to RM.

c. Near-storm environment

STP exhibited the most utility in discriminating tornado environments as a diagnostic parameter amongst a 39-variable database at the SPC, so results from other parameters are not shown. Using either the grid hour or max neighborhood grid hour value (i.e., within 185 km) at the event start location, a similar relationship exists among the STP distributions. RM events tend to exhibit higher STP values than QLCS for the same EF-scale damage rating (Figs. 8–9). In contrast to Vrot, STP for both RM and QLCS exhibit little difference between EF0, EF1, and EF2 distributions for the same mode category. Higher values of STP (i.e., $\geq$ 6) are common for a greater proportion of RM events at higher EF-scale rating classes (i.e., EF3 to $\geq$EF4). It must be stressed that using composite indices such as the STP should not be examined alone but rather in concert with the individual components in the STP that identify important supercell tornado ingredients.

d. Max Vrot—STP—convective mode relationship

Very few ≥ EF3 events occurred with relatively weak Vrot (i.e., < 40 kt) (Fig. 10, lower left) as compared to stronger velocity (i.e., > 50 kt). Weakly damaging tornado events primarily occupy the distribution space featuring weaker velocities and low STP values. Strong tornadoes (i.e., EF2-EF3) tend to mostly occur with Vrot $\geq$ 30 kt but across much of the STP parameter space (e.g., 0.5–15). Violent tornadoes ($\geq$EF4) were found to favor both strong Vrot ($\geq$ 55 kt) and appreciable STP (> 4). Similar to findings by S12, RM comprised a large majority of strong tornado events —compared to QLCS and disorganized storm modes— and displayed a tendency for higher EF damage rating as Vrot increased from 30 kt to $\geq$ 60 kt (Fig. 11). A smaller relative proportion of RM tornado events occurred in the weak Vrot – low STP distribution; conversely, this is where the majority of both tornadic QLCS and disorganized storms occur in the 2-D phase space (c.f., Figs. 11–13).

Tornadic RM storms had a much higher mean STP values than QLCS and disorganized storms, and QLCS had much higher STP values than disorganized storms. Statistically significant differences in STP values were found between $\geq$EF4, EF3, and EF2 RM EF-scale classes using a two-sample tailed difference of means T-test (), which compliments findings by Brotzge et al. (2012) from a similar independent dataset.

e. Conditional tornado probabilities

A conditional probability relationship between Vrot and STP was examined for this dataset. Given a RM, tornado damage intensity probabilities were calculated and compared to a reference climatology (i.e. from the Vrot sample). Stronger Vrot velocity yielded greater conditional probabilities for $\geq$ EF1 tornadoes (Fig. 14). As Vrot increased from 15 kt (i.e., sample climatology) to 40 kt, the conditional probability for $\geq$ EF1 tripled regardless of STP value. Given that a tornado is occurring with a RM, a similar overall trend of increasing conditional probabilities with increasing Vrot was evident (Fig. 15) and little contribution by STP. An analogous trend was noted for $\geq$ EF2 events with Vrot largely contributing to the increase in conditional tornado probabilities compared to STP (Figs. 16–17). STP and Vrot both contributed to greater conditional probabilities for $\geq$ EF3 tornadoes as Vrot and STP increased (Figs. 18–19) and is in contrast to weaker tornado events.

4. Discussion

As part of a comprehensive convective mode–environment investigation at the SPC, both previous foundational studies (i.e., S12 and T12) highlighted the relationship between convective mode, mesocyclone strength, and tornado damage ratings. Additionally, T12 combined near-storm environment data (e.g., STP) to a large sample of tornado events and robustly revealed that high STP, RM convective mode, and strong mesocyclones yielded the greatest combination of ingredients for EF3 $\geq$ tornadoes. However, T12 found substantial overlap in STP distributions by EF-scale rating (T12, their Fig. 12) and emphasized the following statement: *"confident delineation in damage categories will prove difficult for individual storms during a particular hour based on storm mode and environment alone"*. This assertion served as the primary motivation to 1) manually develop a dataset with

greater precision (e.g., 1 kt rotational velocity increments vs. categorized mesocyclone strength) of parent tornadic storm low-level circulation intensity than was done previously in S12. This was completed using the peak lowest level (0.5 deg) velocity data, and differences in tornado events based on EF-scale were examined. This study preliminarily demonstrated the usefulness of a multiple dataset approach to better assess conditional tornado maximum EF-scale probabilities by combining separate information on the near-storm environment, convective mode, and Vrot Fig. 20). Evaluating a conditional tornado threat in this manner may offer additional value-added information in a real-time operational decision-making setting (i.e., warnings). In addition, this approach may be applied in a quasi-steady state scenario in which some short term (e.g., 30 min–2 hr) tornado threat guidance can be linearly extrapolated to assess maximum tornado EF-scale intensity risk. This is one possible approach in moving toward the Warn-On-Forecast concept.

Future work will include continued expansion of the database on a yearly basis in addition to assigning Vrot data to 2009-2010 EF0-EF1 tornado events. Additional work will involve exploring the utility of associating the Vrot database to Warning Decision Support System–Integrated Information (WDSS-II; Lakshmanan et al. 2007) low-level rotation track data (i.e., 0–2 km AGL merged azimuthal shear) in association with the multi-year reanalysis of remotely sensed storms (MYRORSS) project (Cintineo et al. 2011). Possible Research-to-Operations (R2O) may include 5 minute updated objective automated conditional maximum tornado damage rating probability guidance in a gridded format.

ACKNOWLEDGEMENTS

The authors thank Steven Weiss (SPC) for providing valuable input during the early stages of developing the SPC convective mode–environment database. This manuscript benefitted from a review by Israel Jirak (SPC).

REFERENCES

Andra, D. L., 1997: The origin and evolution of the WSR-88D mesocyclone recognition nomogram. Preprints, *28th Conf. on Radar Meteor*., Austin, TX, Amer. Meteor. Soc., 364–365.

Benjamin, S. G., and Coauthors, 2004: An hourly assimilation-forecast cycle: The RUC. *Mon. Wea. Rev*., **32**, 495–518.

Bothwell, P. D., J. A. Hart, and R. L. Thompson, 2002: An integrated three-dimensional objective analysis scheme in use at the Storm Prediction Center. Preprints, *21st Conf. on Severe Local Storms*, San Antonio, TX, Amer. Meteor. Soc., J117–J120.

Brady, R. H., and E. J. Szoke, 1989: A case study of nonmesocyclone tornado development in northeast Colorado: similarities to waterspout formation. *Mon. Wea. Rev.*, **117**, 843–856.

Brooks, H. E., 2009: Proximity soundings for Europe and the United States from reanalysis data. *Atmos. Res.,* **93**, 546–553, doi:10.1016/j.atmosres.2008.10.005

Brotzge, J. A., S. E. Nelson, R. L. Thompson, and B. T. Smith, 2012: Tornado probability of detection and lead time as a funcition of convective mode and environmental parameters. Submitted to *Wea. Forecasting*.

Cintineo, J., T. Smith, V. Lakshmanan, and S. Ansari, 2011: An automated system for processing the multi-year reanalysis of remotely sensed storms (MYRORSS). Preprints, *27th Conf. on Interactive Information Processing Systems (IIPS)*, *91st Amer. Meteor. Soc. Annual Meeting*, Seattle, WA, J9.3.

Crum, T. D., R. L. Alberty, and D. W. Burgess, 1993: Recording, archiving, and using WSR-88D data. *Bull. Amer. Meteor. Soc*., **74**, 645–653.

Glass, F. H., 2011: Warning operations and decision making for the St. Louis tornadoes on Good Friday, 22 April 2011. Powerpoint presentation for *36th Annual Meeting, Nat. Wea. Assoc*., Birmingham, AL. 17 Oct. 2011.

Lakshmanan, V., T. M. Smith, G. J. Stumpf, and K. Hondl, 2007: The Warning Decision Support System–Integrated Information. *Wea. Forecasting*, **22**, 596–612.

Madsig, M. A., 2008: New techniques for integrating environmental information with radar base data analysis in National Weather Service warning decision making. Preprints, *24th Conf. on*

Severe Local Storms, Savannah, GA, Amer. Meteor. Soc., P6.10.

Ortega, K. L., and Coauthors, 2012: Overview of the 24 May 2011 tornado outbreak. Preprints, *Special Symposium on Tornado Disasters of 2011,* 92nd Amer. Meteor. Soc. Annual Meeting, New Orleans, LA, J4.2.

ROC, cited 2012: NEXRAD coverage below 10,000 feet AGL. [Available online at http://www.roc.noaa.gov/WSR88D/Maps.aspx.]

Smith, B. T., R. L. Thompson, J. S. Grams, and J. C. Broyles, 2012: Convective modes for significant severe thunderstorms in the contiguous United States. Part I: Storm classification and climatology. *Wea. Forecasting*, **27**, 1114–1135.

Stensrud, D. J., J. V. Cortinas Jr., and H. E. Brooks, 1997: Discriminating between tornadic and nontornadic thunderstorms using mesoscale model output. *Wea. Forecasting,* **12,** 613–632.

_____, and Coauthors, 2009: Convective scale warn-on-forecast system: A vision for 2020. *Bull. Amer. Meteor. Soc.*,**90**, 1487–1499.

Stumpf, G. J., A. Witt, E. D. Mitchell, P. L. Spencer, J.T. Johnson, M. D. Eilts, K. W. Thomas, and D. W. Burgess, 1998: The National Severe Storms Laboratory mesocyclone detection algorithm for the WSR-88D. *Wea. Forecasting*, **13**, 304–326.

Thompson, R. L., R. Edwards, J.A. Hart, K.L. Elmore and P.M. Markowski, 2003: Close proximity soundings within supercell environments obtained from the Rapid Update Cycle. *Wea. Forecasting*, **18**, 1243–1261.

_____, C. M. Mead, and R. Edwards, 2007: Effective Storm-Relative Helicity and Bulk Shear in Supercell Thunderstorm Environments. *Wea. Forecasting*, **22**, 102–115.

_____, B. T. Smith, J. S. Grams, and C. Broyles, 2012: Convective modes for significant severe thunderstorms in the contiguous United States. Part II: Supercell and QLCS tornado environments. *Wea. Forecasting*, **27**, 1136–1154.

Torres, S. M., and C. D. Curtis, 2007: Initial implementation of super-resolution data on the NEXRAD network. Preprints, *23rd Int. Conf. on Interactive Information Processing Systems,* San Antonio, TX, Amer. Meteor. Soc., 5B.10. [Available online at http://ams.confex.com/ams/pdfpapers/116240.pdf.]

Trapp, R. J. and M. L. Weisman, 2003: Low-Level Mesovortices within Squall Lines and Bow Echoes. Part II: Their Genesis and Implications. *Mon. Wea. Rev.*, **131**, 2804–2823.

——, S. A. Tessendorf, E. S. Godfrey, and H. E. Brooks, 2005: Tornadoes from squall lines and bow echoes. Part I: Climatological distribution. *Wea. Forecasting*, **20**, 23–34.

Wilks, D.S., 2006. Statistical Methods in the Atmospheric Sciences, 2nd Ed. International Geophysics Series, Vol. 59, Academic Press, 627 pp.

Table 1. Mean (median) values of Vrot and STP [effective layer (max value within 185 km)] for RM tornado events by EF-scale class.

	RM EF0	RM EF1	RM EF2	RM EF3	RM EF4+
Vrot	38 (36)	44 (43)	50 (50)	64 (62)	77 (73)
STP (eff layer) max 185 km	4.4 (3.5)	5.0 (4.6)	5.1 (4.4)	6.6 (5.9)	10.3 (10.5)

Table 2. Same as Table 1, except for QLCS and disorganized storm mode tornado events.

	QLCS EF0	QLCS EF1	QLCS EF2	Disorganized EF0	Disorganized EF1
Vrot	30 (30)	35 (35)	39 (38)	15 (14)	29 (25)
STP (eff layer) max 185 km	2.3 (1.8)	2.8 (2.6)	3.2 (2.6)	0.7 (0.1)	1.4 (1.4)

Table 3. Mean differences in Vrot and STP [effective layer (max value within 185 km)] for RM. Parameter units are the same. Red boldface differences are statistically significant at $\alpha < 0.001$, and red boldface and italic differences are considered to be sufficiently large to be of operational significance.

	RM EF4+ – RM EF0	RM EF4+ – RM EF1	RM EF4+ – RM EF2	RM EF4+ – RM EF3	RM EF3 – RM EF0	RM EF3 – RM EF1	RM EF3 – RM EF2
Vrot	***39***	***33***	***26***	***13***	***26***	***20***	***13***
STP (eff layer) max 185 km	***6.0***	***5.3***	***5.3***	***3.7***	***2.2***	***1.6***	***1.5***

Table 4. As in Table 3 except for RM–RM and RM–QLCS differences.

	RM EF2 – RM EF0	RM EF2 – RM EF1	RM EF1 – RM EF0	QLCS EF2 – QLCS EF1	QLCS EF2 – QLCS EF0	QLCS EF1 – QLCS EF0	RM EF2 – QLCS EF2
Vrot	***13***	**7**	**6**	**9**	3	**6**	***12***
STP (eff layer) max 185 km	0.7	0.1	0.7	0.8	0.3	0.5	***1.9***

Table 5. As in Table 4.

	RM EF2 – QLCS EF1	RM EF2 – QLCS EF0	RM EF1 – QLCS EF2	RM EF1 – QLCS EF1	RM EF1 – QLCS EF0	RM EF0 – QLCS EF2	RM EF0 – QLCS EF1	RM EF0 – QLCS EF0
Vrot	***15***	***21***	5	***8***	***14***	1	2	***8***
STP (eff layer) max 185 km	***2.2***	***2.8***	***1.9***	***2.2***	***2.7***	**1.2**	***1.5***	***2.0***

Figures

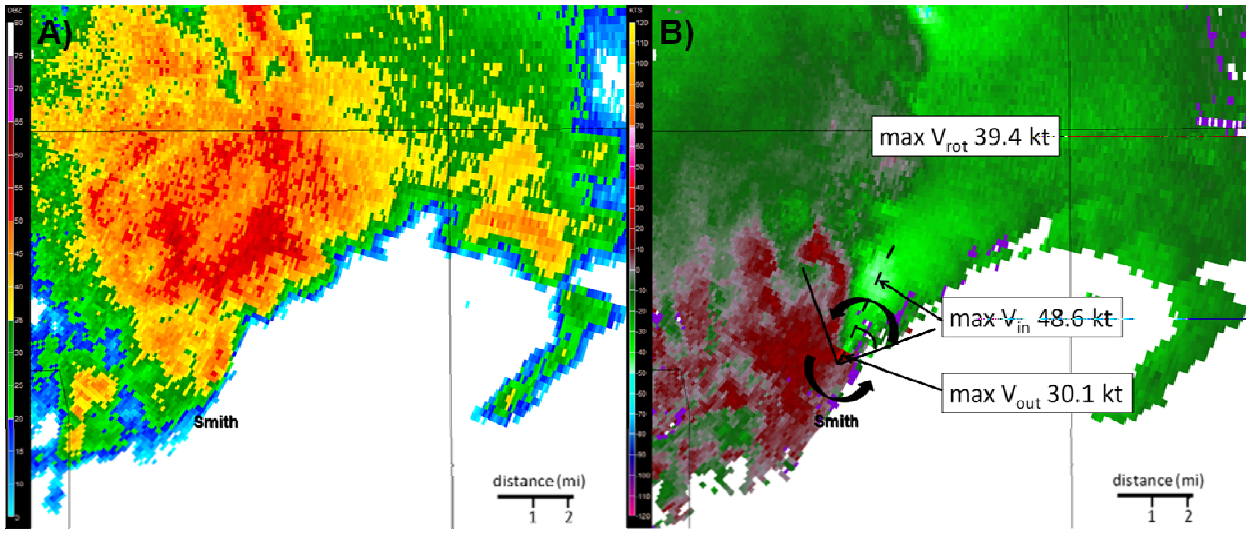

Figure 1. A) WSR-88D base reflectivity (dBZ, color scale on left) at 0.5º beam tilt from Jackson, MS (KDGX) at 0852 UTC on 30 November 2010. A cluster RM produced an EF2 tornado in Smith County MS (start time 0844 UTC). North is up; county borders are black; distance scale (lower right). **B)** Same as Fig. 1A, except for storm relative velocity (kt, scale on left), 45 degree angle insert, and curved arrows signifying rotation. Denoted inserts display maximum inbound storm relative velocity (max V_{in}, 48.6 kt), maximum outbound storm relative velocity (max V_{out}, 30.1 kt), maximum rotational velocity (max V_{rot}, 39.4 kt).

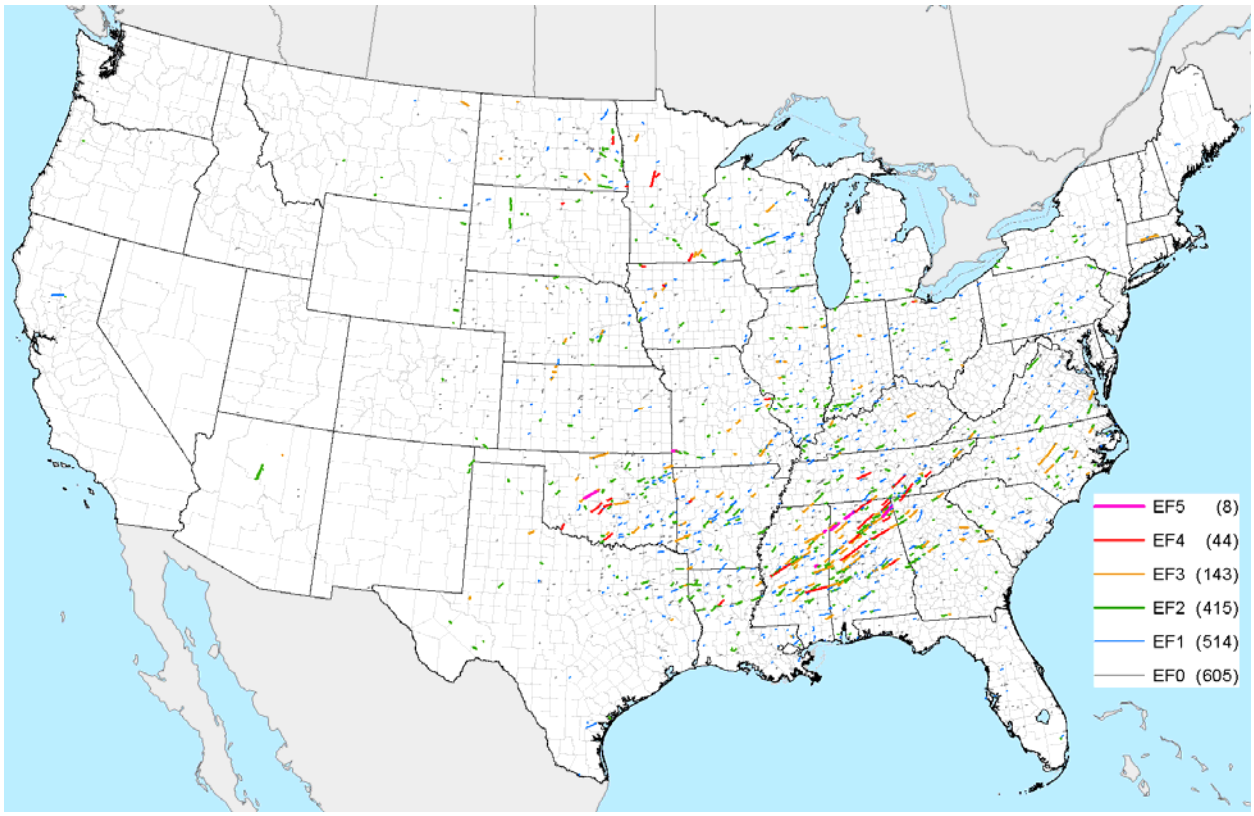

Figure 2. Spatial plot of events where V_{rot} > 0 kt.

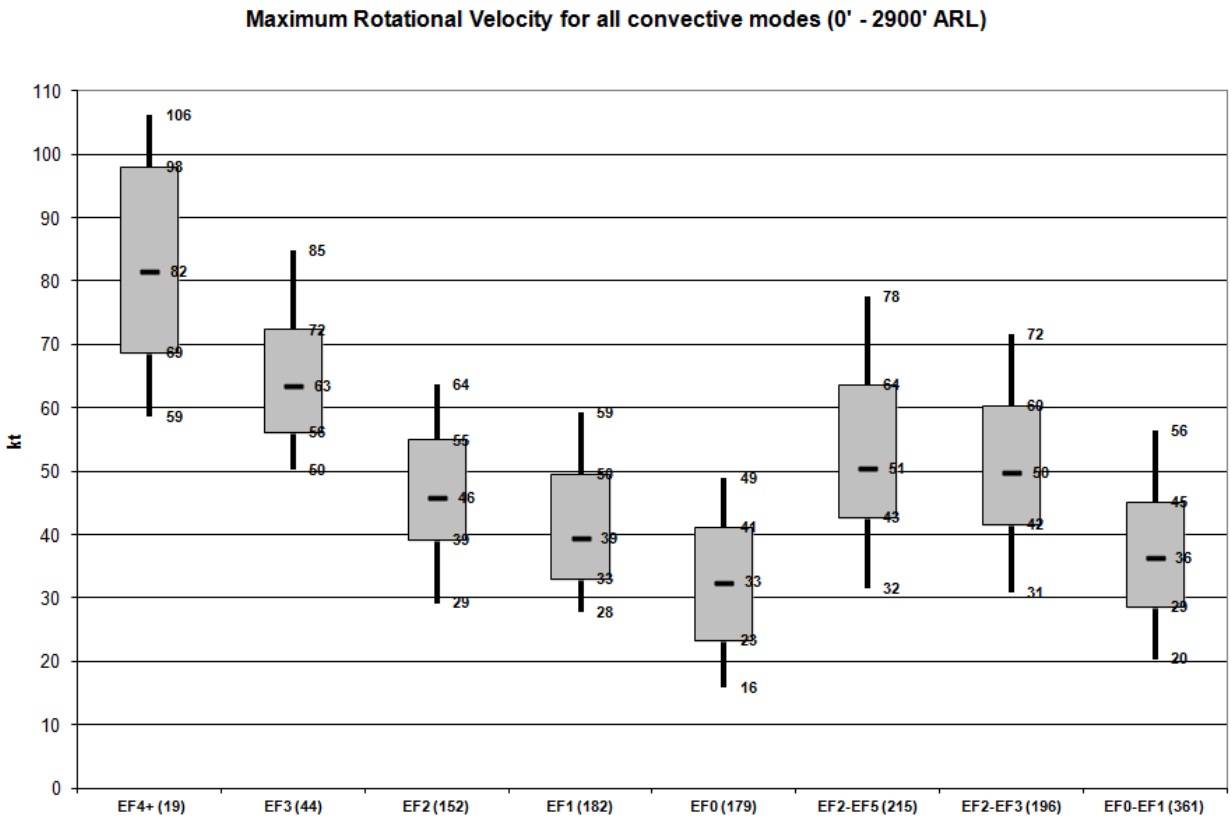

Figure 3. Maximum rotational velocity (V_{rot}) for all convective mode tornado events [0' – 2900' above radar level (ARL)].

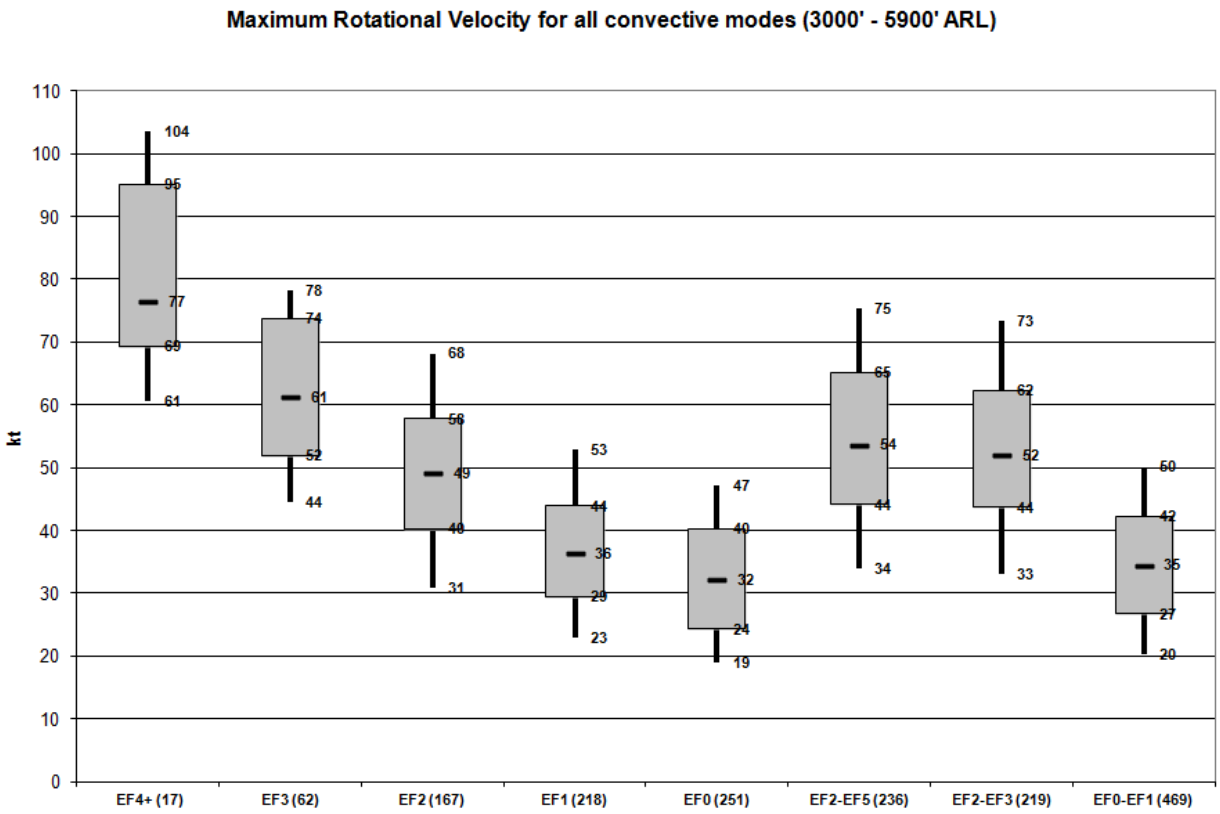

Figure 4. Same as Fig. 3 except for tornado events 3000’ – 5900’ ARL.

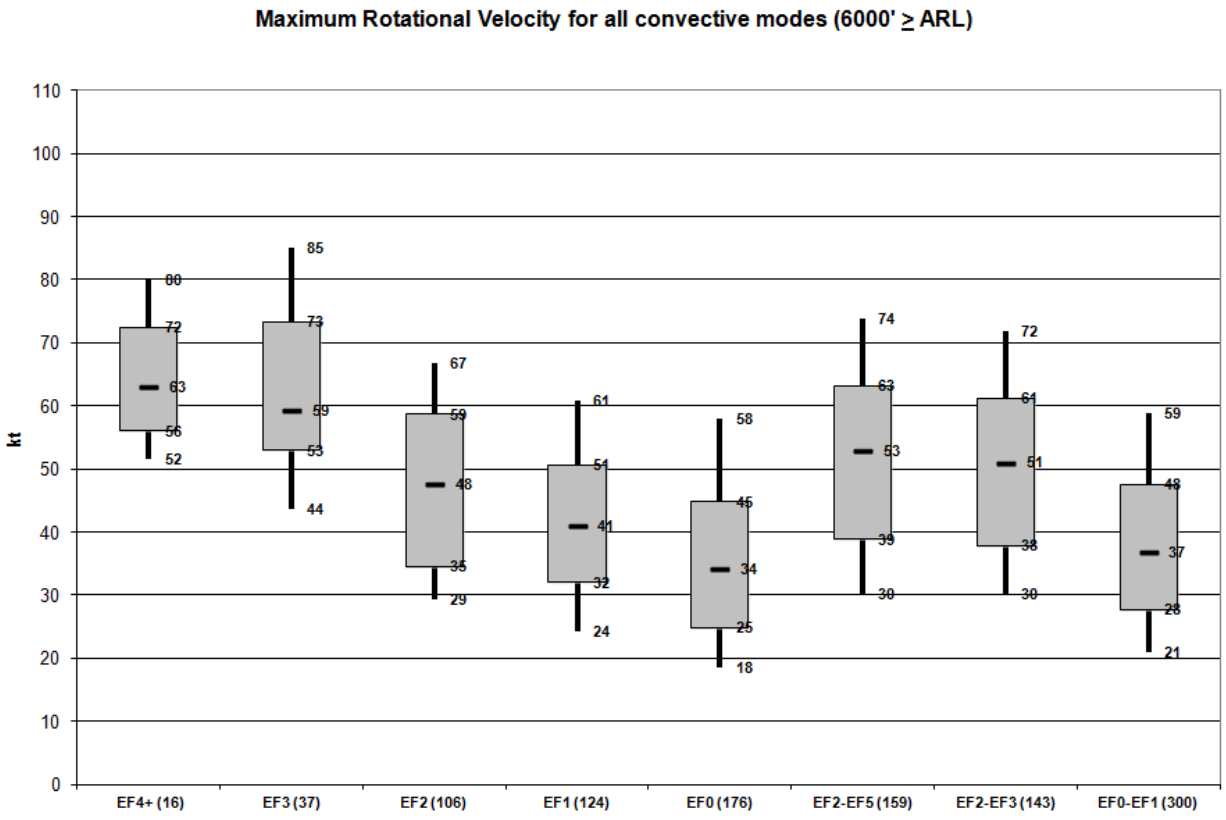

Figure 5. Same as Fig. 3 except for tornado events ≥ 6000’ ARL.

Figure 6. NEXRAD coverage at or above 3000 ft, 6000 ft ARL. The level refers to the center of the beam height (assuming standard atmospheric refraction). Terrain blockage indicated where 50% or more of the beam is blocked.

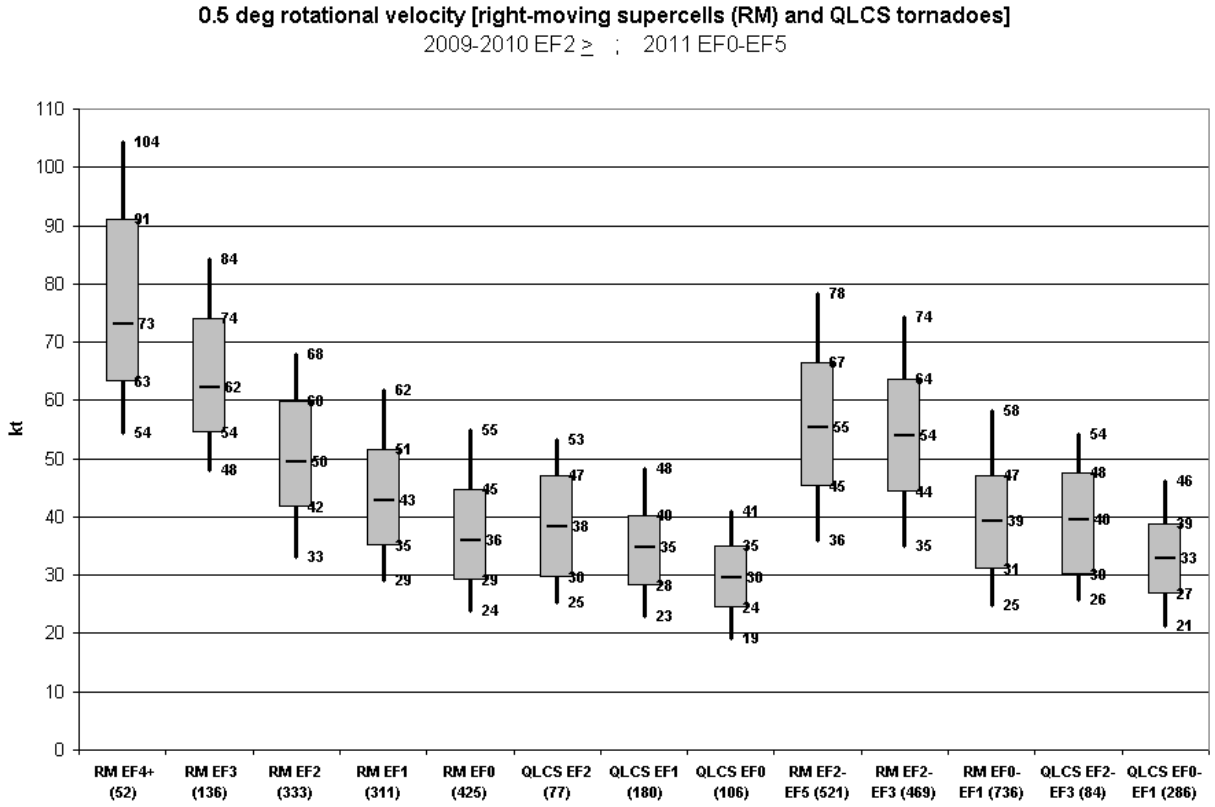

Figure 7. Box and whiskers plot of 0.5 degree peak rotational velocity (kt) from ≥ EF2 2009-2010; and EF0-EF5 2011 tornadoes grouped by right-moving supercell (RM) and QLCS. The shaded boxes span the 25th to the 75th percentiles, and the whiskers extend upward to the 90th and downward to the 10th percentiles. Median values are marked within the box, and sample sizes for each storm mode are shown in parentheses.

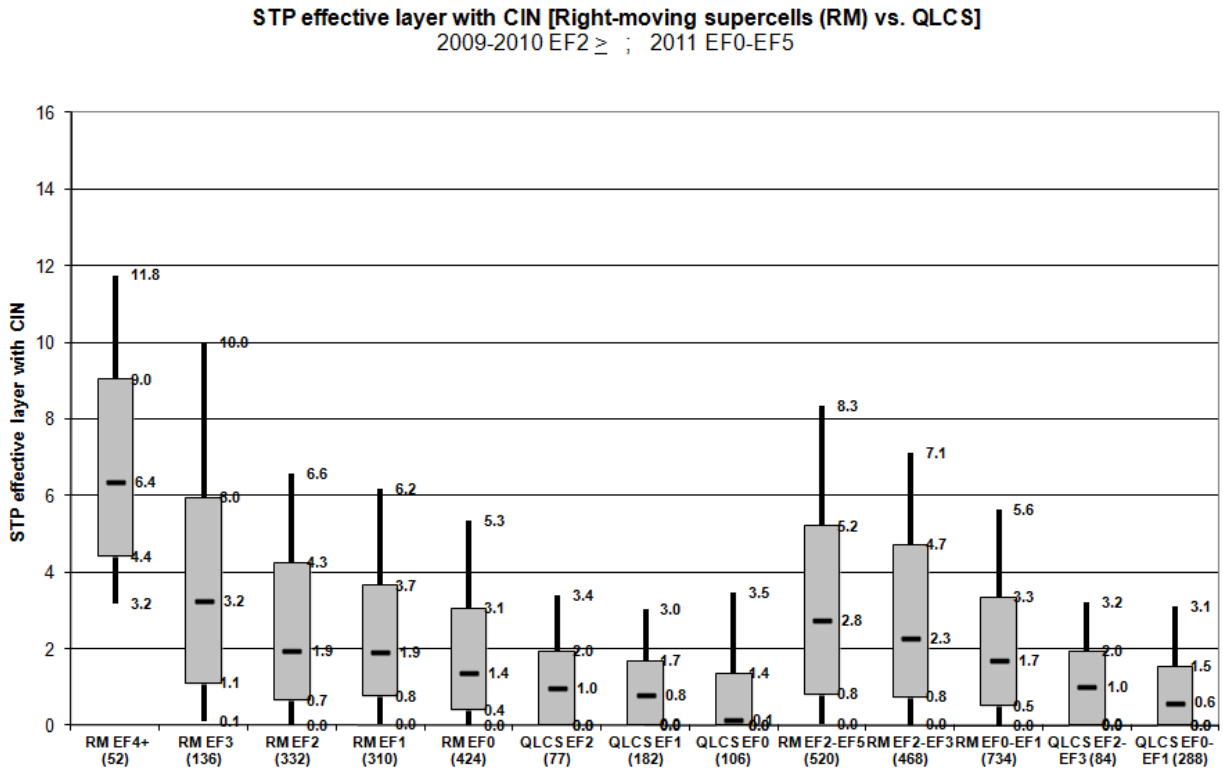

Figure 8. As in Fig. 7, but for the significant tornado parameter (STP) effective layer (grid value).

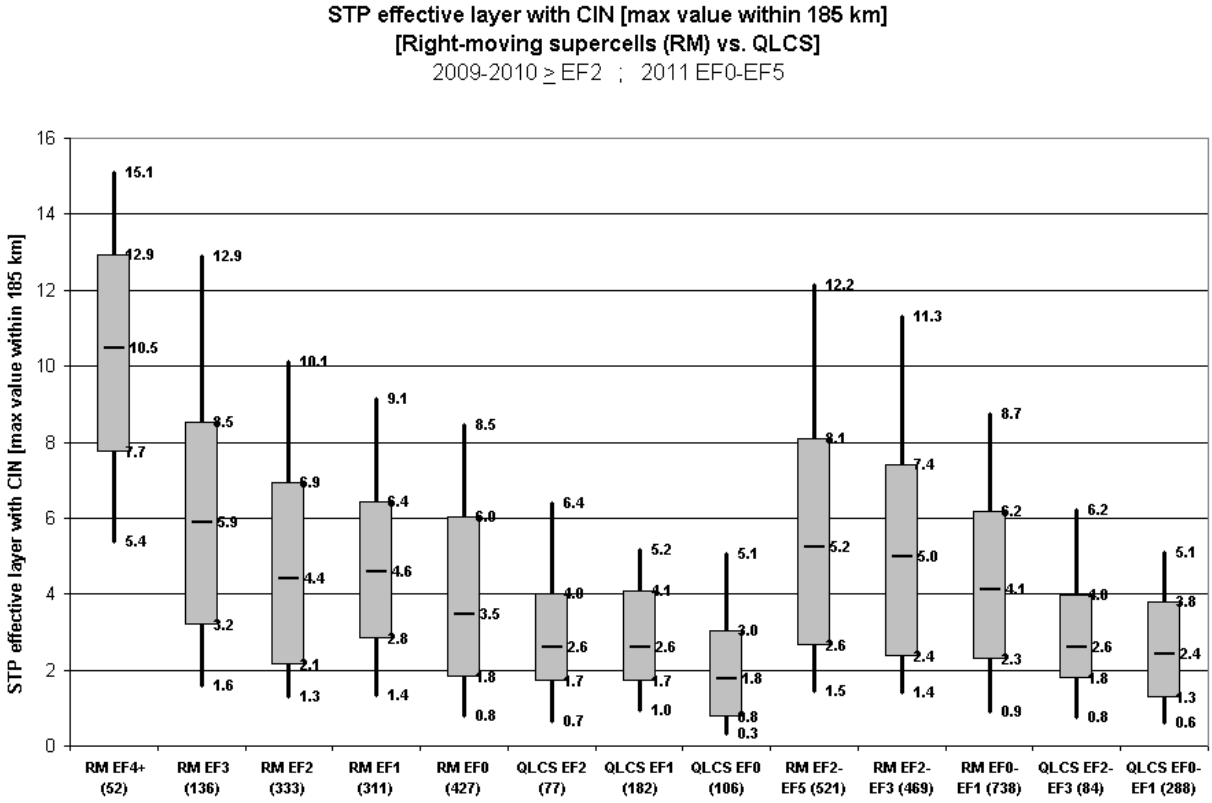

Figure 9. As in Fig. 7, but for the significant tornado parameter (STP) effective layer (max value within 185 km).

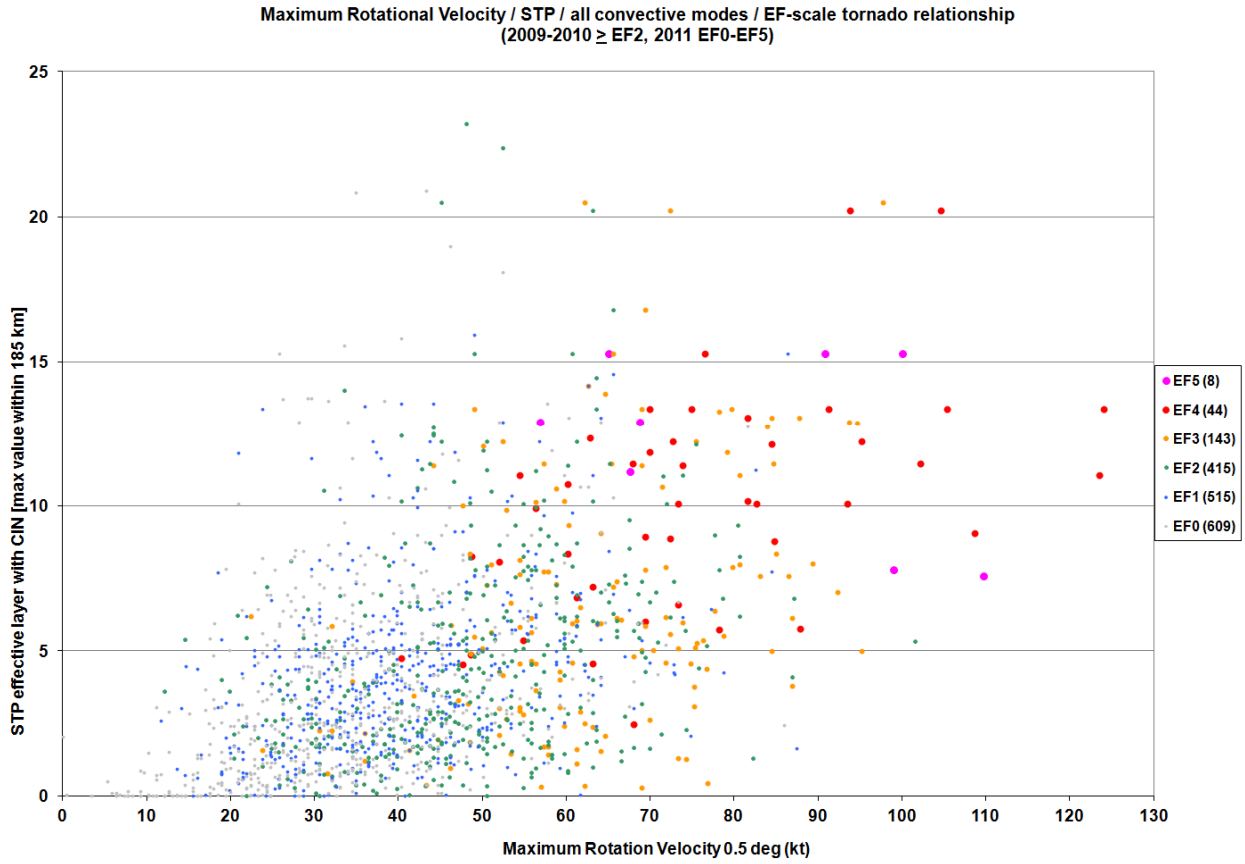

Figure 10. Scatterplot of ≥ EF2 2009-2010 and 2011 EF0-EF5 tornado events by EF-scale rating (legend; middle right) of 0.5 degree peak rotational velocity (kt) x-coordinate vs. STP effective layer (max value within 185 km).

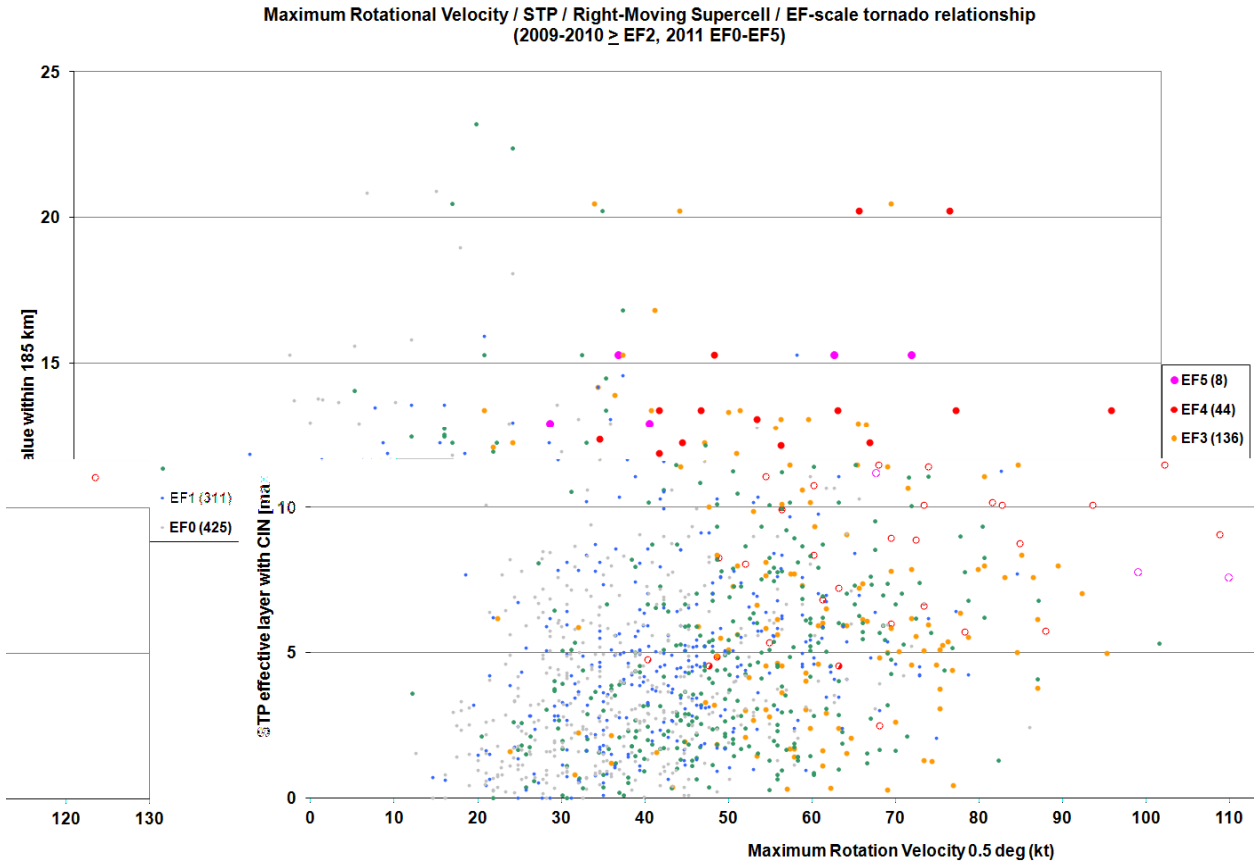

Figure 11. As in Fig. 10 except for RM.

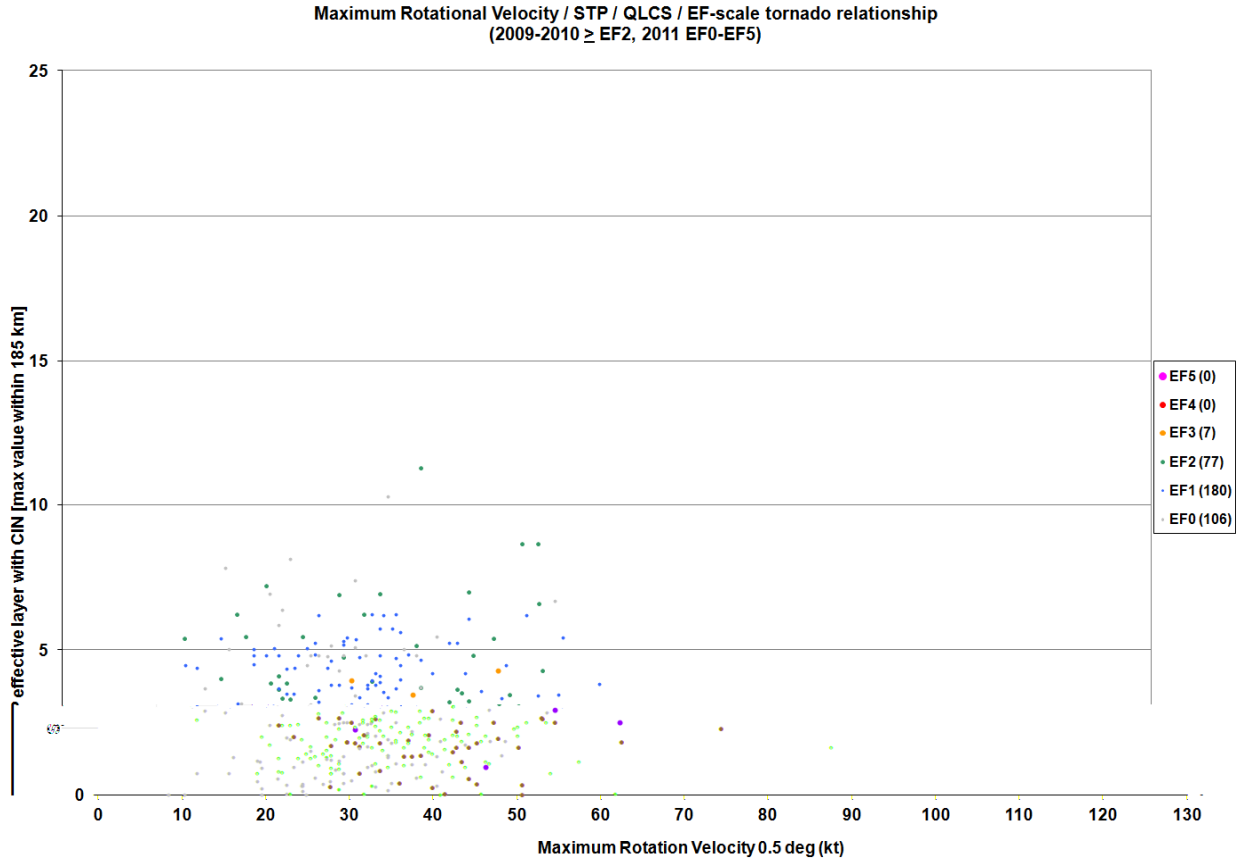

Figure 12. As in Fig. 10 except for QLCS.

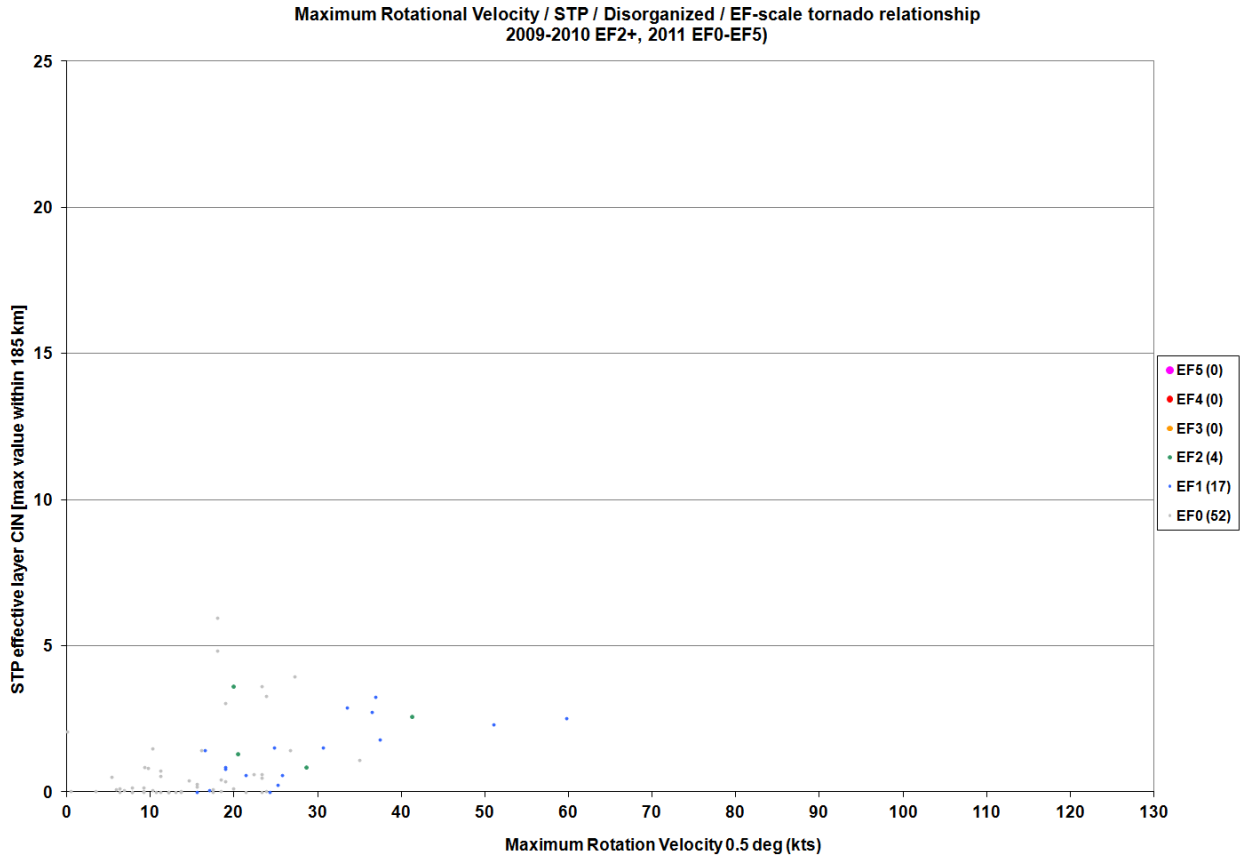

Figure 13. As in Fig. 10 except for disorganized storms.

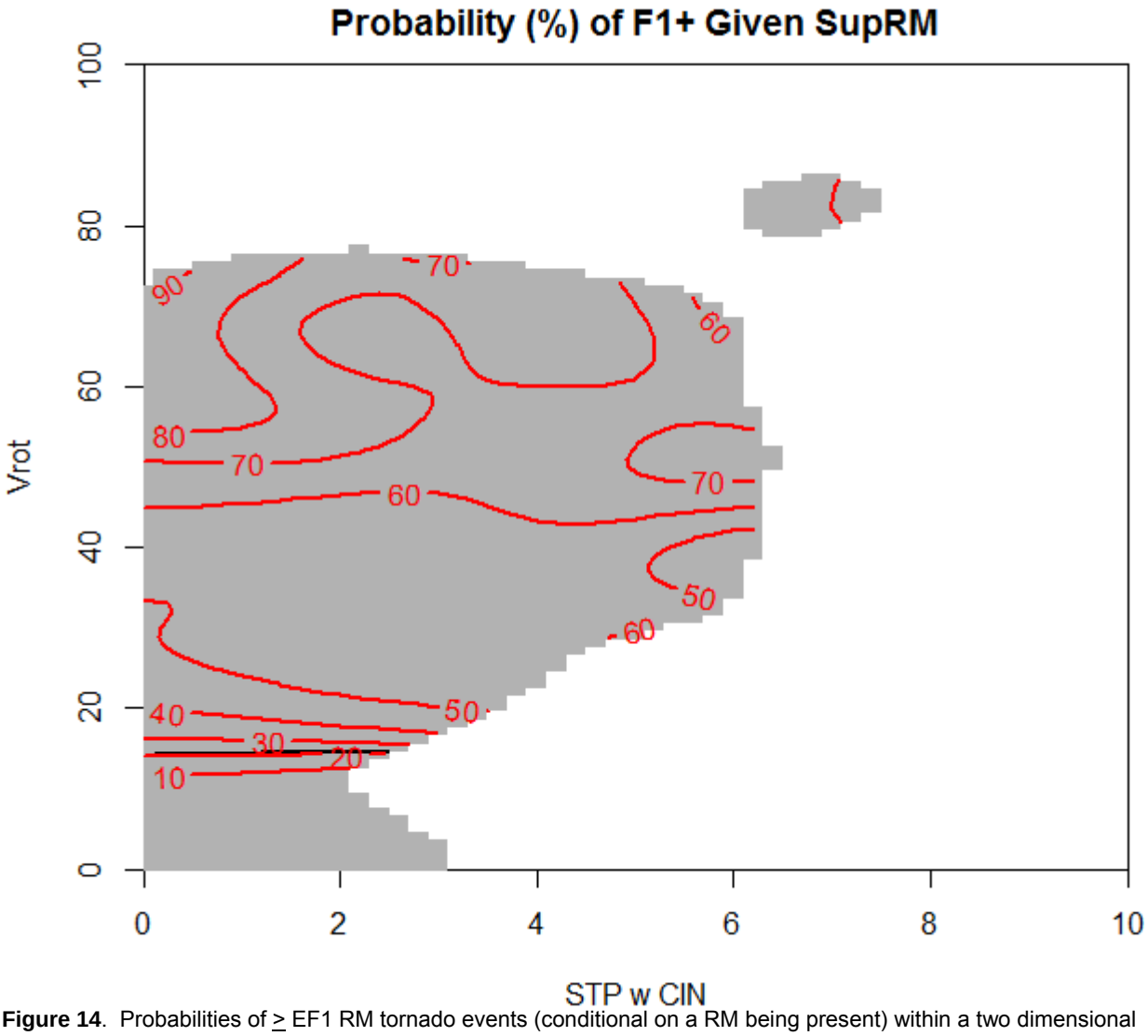

Figure 14. Probabilities of ≥ EF1 RM tornado events (conditional on a RM being present) within a two dimensional phase space for STP effective layer with CIN (x-axis) and Vrot (y-axis) using a two-dimensional Gaussian kernel. Gray area indicates where there is a large enough density, subjectively determined, to warrant calculating probabilities. The location of the climatological probability for the sample climatology is indicated by a black line and departures from that sample climatology are what should be considered.

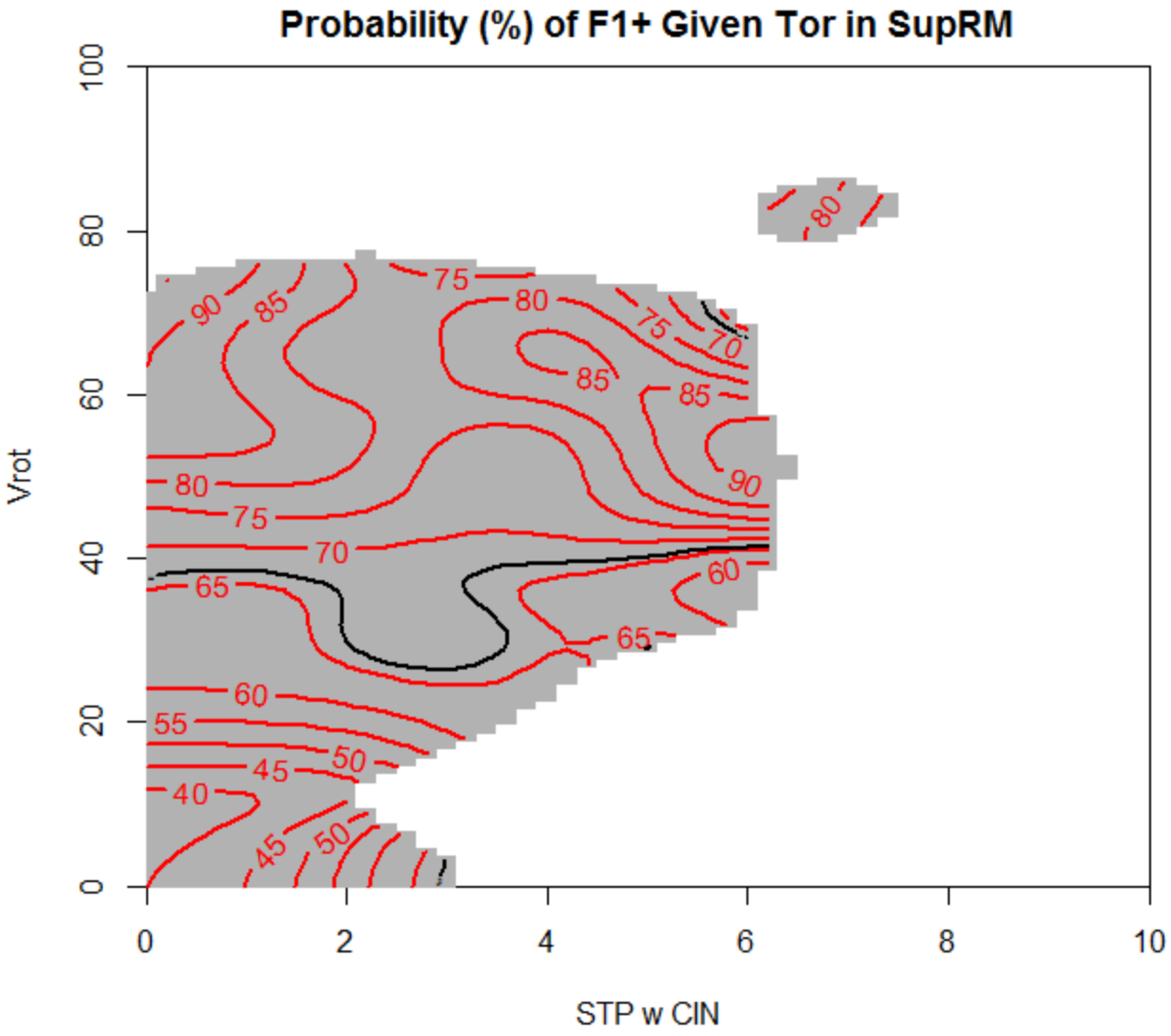

Figure 15. As in Fig. 14 except for a ≥ EF1 RM tornado present.

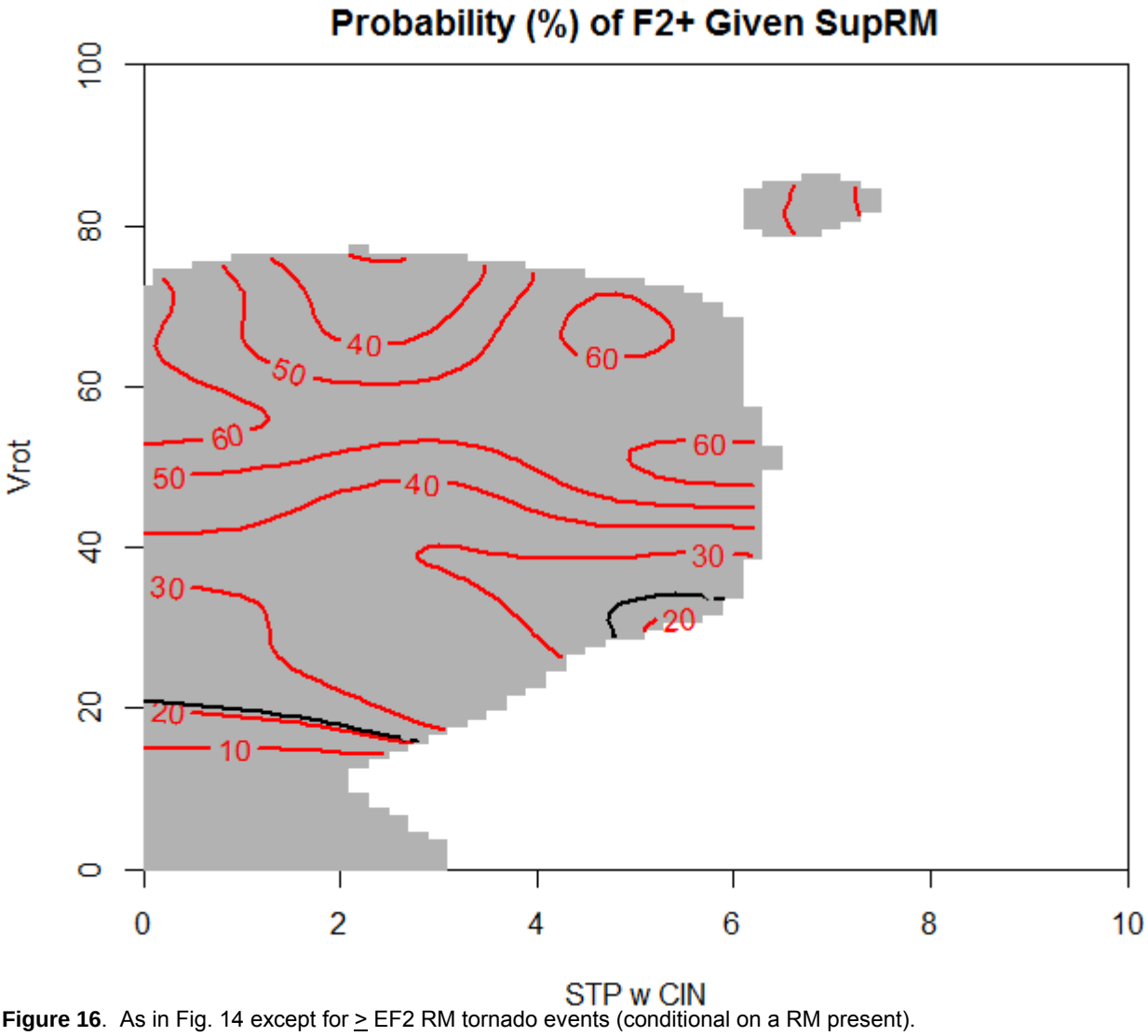

Figure 16. As in Fig. 14 except for ≥ EF2 RM tornado events (conditional on a RM present).

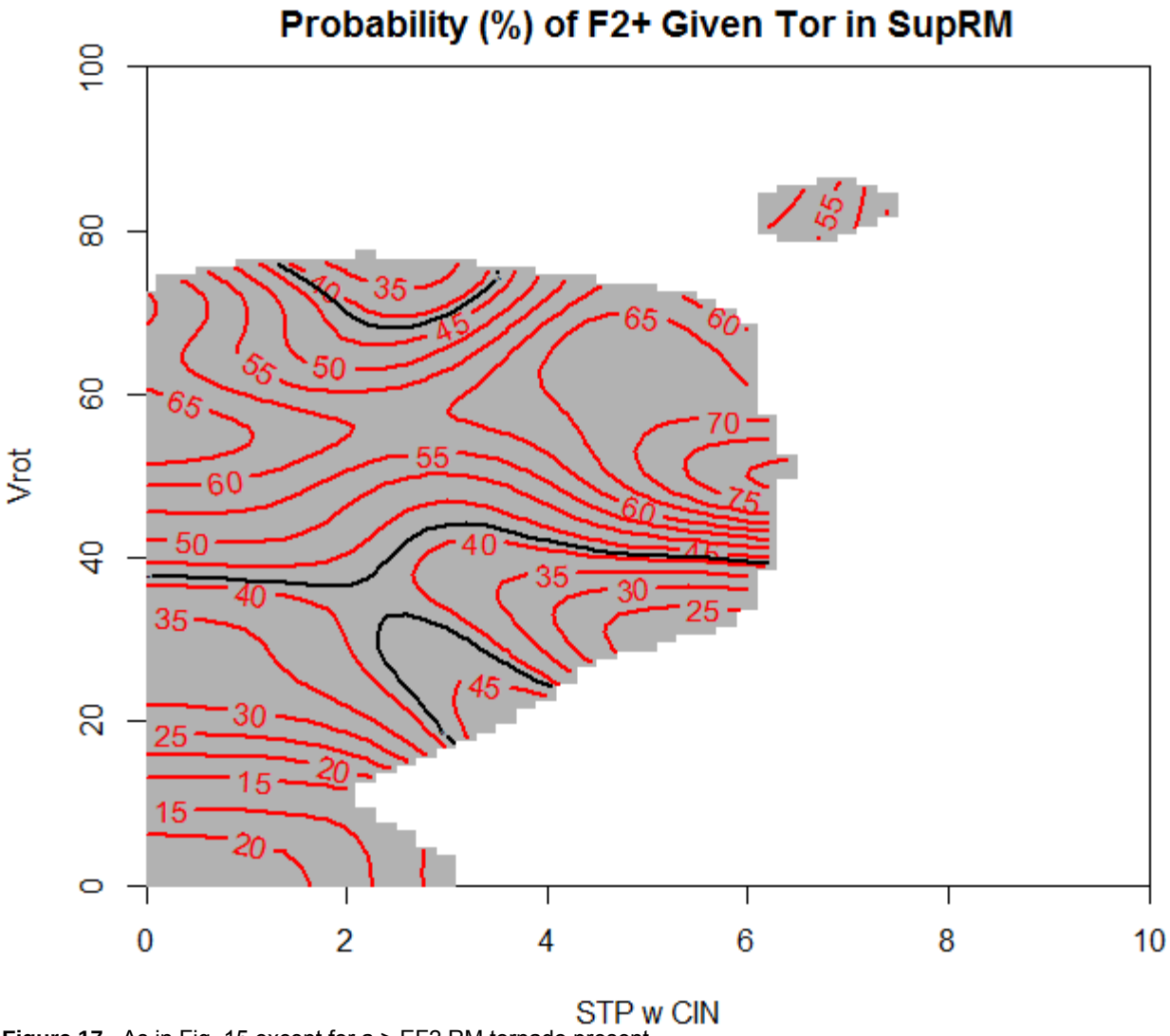

Figure 17. As in Fig. 15 except for a ≥ EF2 RM tornado present.

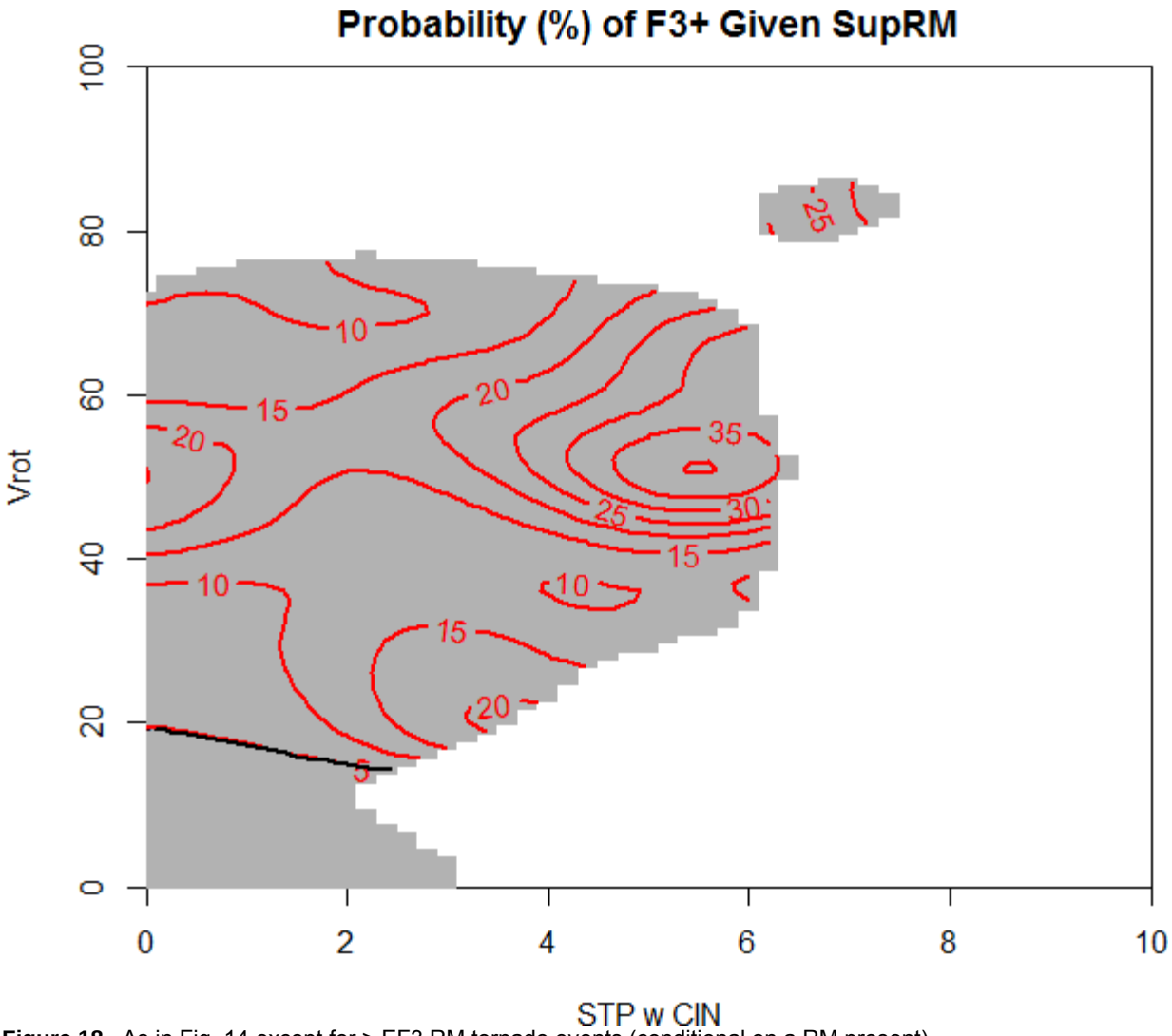

Figure 18. As in Fig. 14 except for ≥ EF3 RM tornado events (conditional on a RM present).

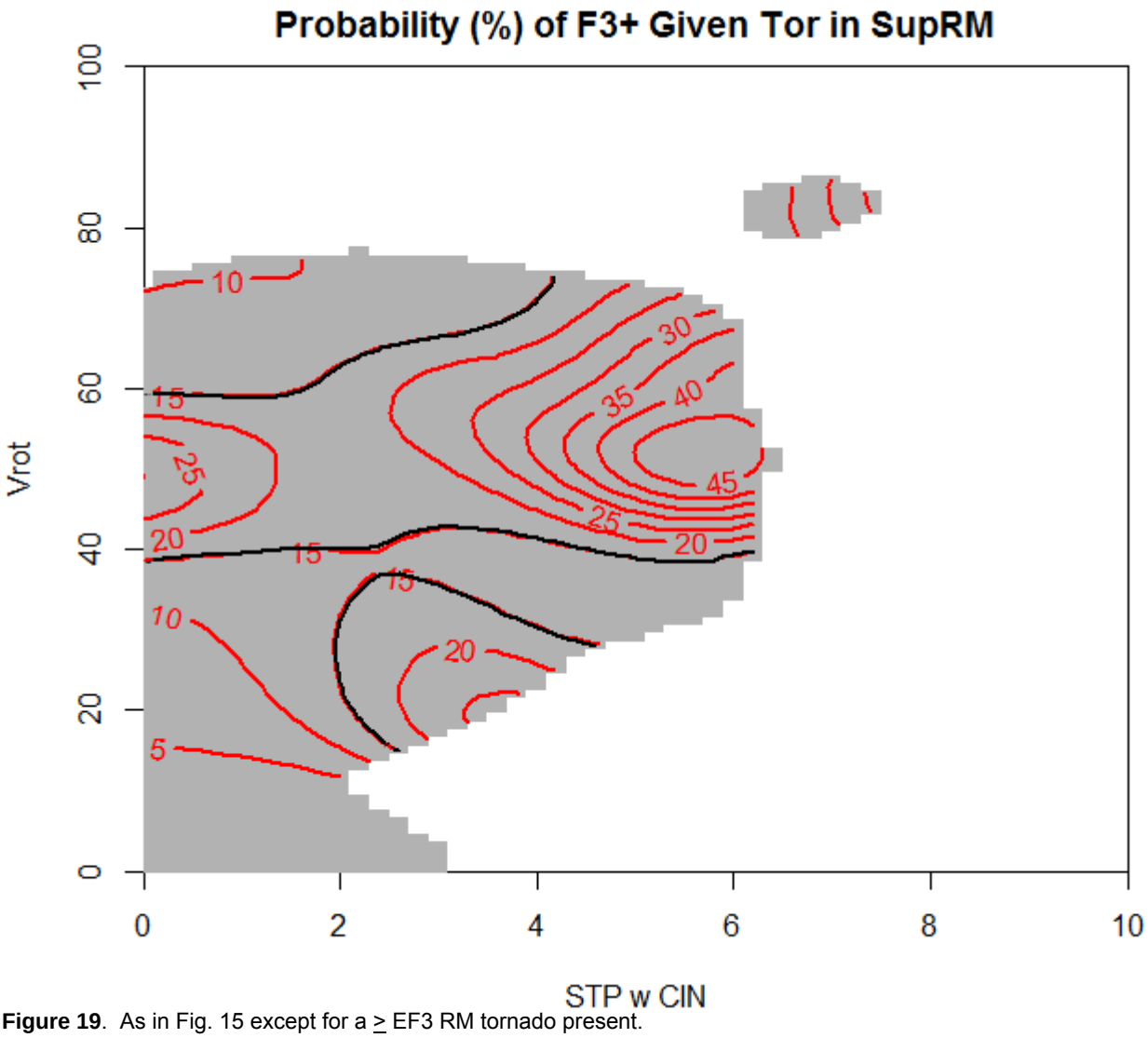

Figure 19. As in Fig. 15 except for a ≥ EF3 RM tornado present.

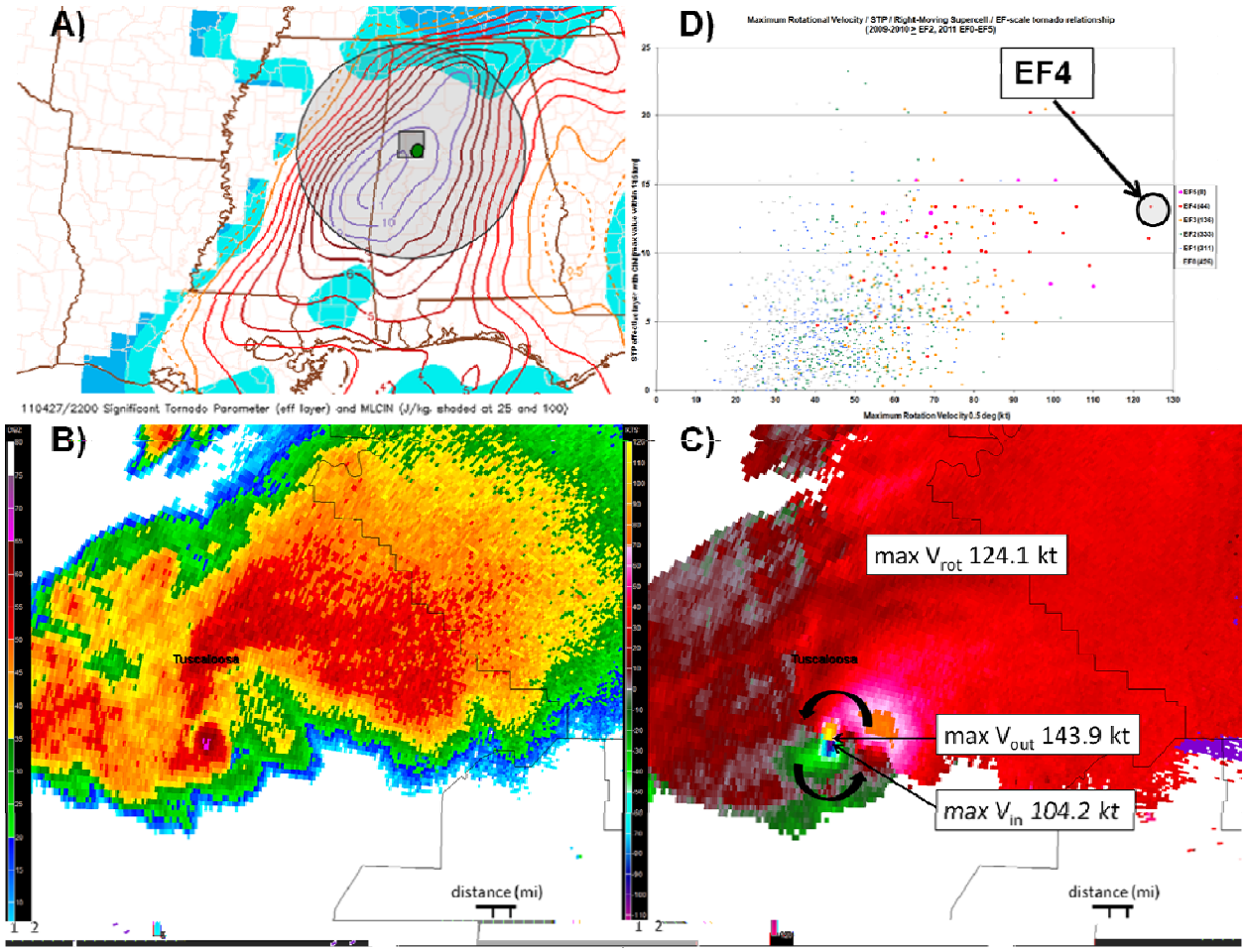

Figure 20. **A)** Planar view of STP (effective layer with CIN) at 2200 UTC on 27 April 2011. Tuscaloosa, AL EF4 tornadic storm location (green circle), SPC mesoanalysis 40 km grid (black square), and 185 km radius (black circle). Note: smoothed planar max STP value (11-12) is different than max grid value (13.3). **B)** As in Fig. 1 except from Birmingham, AL (KBMX) at 2219 UTC on 27 April 2011. A cluster RM produced an EF4 tornado in Tuscaloosa County AL. **C)** As in Fig. 1B, except for maximum inbound storm relative velocity (max V_{in}, 104.2 kt), maximum outbound storm relative velocity (max V_{out}, 143.9 kt), maximum rotational velocity (max V_{rot}, 124.1 kt). **D)** As in Fig. 11 with the event highlighted (black circle) on the Vrot—STP—RM scatterplot distribution.